

Article

Effect of Al₂O₃ on Inclusion Removal in H13 Steels Using High-Basicity LF (Ladle Furnace) Refining Slags

Ting Liang ¹, Zhuo Qin ¹ and Linzhu Wang ^{2,*}

¹ College of Materials and Metallurgy, Guizhou University, Guiyang 550000, China; tliang2002@outlook.com (T.L.); zqing1945@outlook.com (Z.Q.)

² College of Metallurgical and Ecological Engineering, University of Science and Technology Beijing, Beijing 100083, China

* Correspondence: lzwang@gzu.edu.cn; Tel.: +86-152-8607-0559

Abstract: In this experiment, a quaternary fluorine-free refining slag system of CaO-SiO₂-Al₂O₃-MgO was selected, with basicity ratios of 2, 4, and 6 and calcium-aluminum ratios of 1.5, 2.1, and 3. High-temperature “slag-steel equilibrium” experiments were conducted to investigate the influence of different basicity ratios and calcium–aluminum ratios on the morphologies, compositions, sizes, and quantities of the inclusions in H13 steel, aiming to improve the cleanliness of H13 steel to meet practical industrial requirements. The experimental results showed that with the increase in the basicity ratio and the calcium–aluminum ratio, the morphologies of the inclusions changed from elliptical to regular circular, with more regular edges. As the basicity ratio increased from 2 to 6, the densities of the inclusions showed a decreasing trend, with values of 40, 35, 30, 25, 32, and 30 inclusions/mm². When the basicity ratio remained the same, the average size of the inclusions in the steel decreased first and then increased with the increases in the calcium–aluminum ratios, with sizes of 1.59 μm, 1.23 μm, and 1.38 μm, respectively. Among these, when the basicity ratio was 6 and the calcium–aluminum ratio was 2.1, the control effect on the densities and sizes of the inclusions was the best, yielding an inclusion density of 25 inclusions/mm² and a size of 1.15 μm. Additionally, reducing the Al₂O₃ content in the slag could reduce the Al₂O₃ contents in the inclusions, which also promoted improvements in the elastic deformation capacities of the inclusions. With increases in the calcium–aluminum ratios in the slag system, the masses of the inclusions decreased due to the reduced Al contents in the steel. The Al contents in the steel also had an impact on the compositions of the inclusions.

Keywords: H13 steel; fluorine-free refining slag; alkali ratio; calcium–aluminum ratio; inclusions



Citation: Liang, T.; Qin, Z.; Wang, L. Effect of Al₂O₃ on Inclusion Removal in H13 Steels Using High-Basicity LF (Ladle Furnace) Refining Slags. *Metals* **2023**, *13*, 1592. <https://doi.org/10.3390/met13091592>

Academic Editor: Alexios P. Douvalis

Received: 2 August 2023

Revised: 1 September 2023

Accepted: 12 September 2023

Published: 14 September 2023



Copyright: © 2023 by the authors. Licensee MDPI, Basel, Switzerland. This article is an open access article distributed under the terms and conditions of the Creative Commons Attribution (CC BY) license (<https://creativecommons.org/licenses/by/4.0/>).

1. Introduction

Hot work tool steels are mainly used to manufacture molds for metal or liquid metal pressing above recrystallization temperatures, such as hammer forging molds, die forging molds, hot extrusion molds, and die casting molds [1]. According to the amounts of alloying elements, hot work tool steels can be classified into low-alloy hot work tool steels, medium-alloy hot work tool steels, and high-alloy hot work tool steels. H13 steel is currently the most widely used medium-alloy hot work tool steel. Since its development, it has been widely studied and applied due to its excellent mechanical properties (high strength, red hardness, high toughness, and good plasticity), as well as its high hardenability and medium-temperature stability, and it is commonly used as a mold for hot extrusion, high-speed precision forging, and aluminum alloy die casting, among others [2]. When using H13 steel, it must withstand the impact and compressive stress of high-temperature molten metal, as well as the tensile stress generated when the cast metal solidifies around it, resulting in complex stress conditions. It often fails due to thermal cracking, overall brittle fractures, corrosion, or erosion. Studies have shown that tool steels are very sensitive to

fatigue and inclusions, especially brittle inclusions, which cause stress concentrations in the steel matrix and are usually important factors affecting the life of a tool steel [3,4]. Therefore, one of the key technologies for producing high-quality tool steels is to improve the cleanliness of H13 steel [5–7] by controlling the compositions, quantities, and size distributions of the inclusions in the steel to improve its performance [8]. At present, the main refining slag systems commonly used in smelting H13 high-strength steel are CaO-SiO₂-Al₂O₃-MgO-CaF₂ quaternary slag systems and CaO-SiO₂-Al₂O₃-MgO quaternary slag systems. Although the addition of CaF₂ can reduce the viscosity of refining slag and improve the effect of refining slag on the removal of inclusions in steel, CaF₂ easily decomposes in high temperature smelting environments, and the toxic vapor it releases causes serious harm to human health, pollutes the environment, and causes air pollution, which is not conducive to environmental protection. Therefore, it is necessary to develop fluorine-free refining slag for smelting iron and steel.

Many scholars have conducted research on the control and removal of inclusions in terms of their compositions and sizes [9], such as the use of calcium treatment to modify inclusions [10–13]. However, the insufficient or excessive addition of calcium can result in high-melting-point inclusions, such as partially modified Al₂O₃ or spinel inclusions, as well as CaS, which worsens the treatment effect [14–18]. Many scholars [19–21] used aluminum deoxidation slag and refining slag with a high desulfurization capacity to remove sulfur from steel. Zhao et al. [22] demonstrated that refining slag can effectively control the plasticity and contents of the O, Al, and S in the inclusions. Wu [23] studied the influence of MgO content in slag on the compositions, sizes, and quantities of inclusions in H13 steel. Through a review of the literature on commonly used slag systems in domestic steel mills, we concluded that it is reasonable to control the basicity ratios of refining slag to within the range of 2–5.5 [24–27].

Yang et al. [28,29] studied the influence of refining slag with basicity ratios of 2.5–4.5 on inclusions in steel and found that the inclusions in the steel were mainly spherical CaO-SiO₂-Al₂O₃-MgO composite inclusions. With increases in the basicity ratios, the quantities and sizes of the inclusions decreased. Wang et al. [30] showed that under the action of high-basicity refining slag, the sizes of Al₂O₃ inclusions, calcium-aluminum silicate inclusions, and sulfide inclusions all decreased significantly. Yu et al. [31] found in their experiments that with increases in the basicity ratios (CaO/SiO₂) of the refining slag from 2 to 4.5, the total quantity, total area, and average radius of the inclusions decreased. Regarding the influence of calcium–aluminum ratios in refining slag on inclusions, Ji et al. [32,33] studied the effects of calcium–aluminum ratios ($w(\text{CaO})/w(\text{Al}_2\text{O}_3)$) in high-basicity refining slag on the cleanliness of steel and inclusions, and they found that with increases in the calcium–aluminum ratios in the slag, the cleanliness of the steel improved.

In summary, we researched CaO-SiO₂-Al₂O₃-MgO quaternary fluorine-free refining slag systems. This experiment studied the influence of a medium-to-high basicity refining slag system with different calcium–aluminum ratios on the compositions, quantities, and sizes of the inclusions in the steel. Ultimately, a refining slag system with good control effects on the compositions, quantities, and sizes of the inclusions in steel was obtained. This study contributes to improving the cleanliness of ingots, controlling the morphologies and sizes of inclusions and carbides in steel, and is of great significance for improving the cleanliness of mold steel ingots, controlling the fine dispersion of inclusions in mold steels, and regulating the morphologies and sizes of carbides in steel to enhance the performance of mold steels.

2. Materials and Methods

2.1. Slag-Steel Equilibrium Experiment

High-temperature “slag-steel equilibrium” experiments were conducted to investigate the influence of refining slag composition on the cleanliness of mold steels. H13 mold steel was selected as the steel grade, and its composition is shown in Table 1. Among them, the main element content in the steel was the O content, which was 0.0022%, and the Al

content was 0.004%. A quaternary slag system of CaO-Al₂O₃-SiO₂-MgO was used as the refining slag, and the initial composition of the refining slag used in the high-temperature “slag-steel equilibrium” experiments with different basicity ratios (2.0~6.0) and CaO/Al₂O₃ ratios (1.5~3.0) (CaO/Al₂O₃ is hereinafter denoted by C/A) is presented in Table 2. The experiments were conducted in a tubular resistance furnace. Steel samples weighing approximately 200 g were measured using a balance, and 80 g of slag material was weighed and placed in an alumina crucible. The slag was stirred with a glass rod and held at 1600 °C for 1 h. After the insulation time, the crucible was immediately removed and water-cooled, followed by the extraction of 20 g of the slag material for analysis. The remainder of the slag sample was used as the experimental pre-melting slag. The mold steel sample was placed in an MgO crucible, heated with an electric current, and protected with argon gas (the argon flow rate was maintained at 0.3 min/L in each furnace). The temperature was raised to 1873 K and held for 10 min until the steel sample was in a fully molten state. The molten steel sample was extracted using a quartz tube and rapidly water-cooled. Subsequently, the experimental pre-melting slag was added to the crucible, and after 60 min of insulation, the crucible was removed and rapidly water-cooled to complete the experiment.

Table 1. Chemical composition of the test steel.

Element	C	Cr	Mo	Si	Al	N	O
Content (%)	0.489	5.367	1.521	0.952	0.004	0.0076	0.0022
Element	P	Mn	Mg	V	S		
Content (%)	0.001	0.364	0.001	0.96	0.0023		

Measurement error: $\pm 0.0001\%$.

Table 2. Initial chemical composition of the refining slag (%).

Experiment Number	CaO	SiO ₂	Al ₂ O ₃	MgO	Basicity	C/A
R1	47.6	23.8	22.6	6	2.0	2.1
R2	54.4	13.6	26.0	6	4.0	2.1
R3	57.2	9.5	27.3	6	6.0	2.1
R4	49.0	12.3	32.7	6	4.0	1.5
R5	59.3	14.8	19.9	6	4.0	3.0

Measurement error: $\pm 0.1\%$.

2.2. Experimental Analysis Methods

The polished steel samples after smelting were subjected to scanning electron microscopy (SEM) analysis. Twenty inclusions were selected from each group of steel samples for energy-dispersive X-ray spectroscopy (EDS) scanning to analyze the compositions of the inclusions. Fifty SEM images were captured at 2000 \times magnification for each group of steel samples, with imaging areas of 0.4 mm², to statistically analyze the area densities and uniformities of the inclusions in the steel. The oxygen and sulfur contents in the steel were determined using a carbon-sulfur analyzer while the magnesium and aluminum contents in the steel were determined using inductively coupled plasma optical emission spectroscopy (ICP-OES) (the measurement error of the experimental instrument was $\pm 0.0001\%$). The compositions of the slag samples before and after the experiments were analyzed using X-ray fluorescence (XRF) (the measurement error of the experimental instrument was $\pm 0.1\%$).

3. Results and Discussion

3.1. Morphologies and Compositions of the Inclusions

The morphologies and compositions of typical inclusions in steel samples are shown in Figure 1. The morphology of an inclusion in H13 steel is ellipsoidal or quasi-spherical, and such inclusions are mainly composed of complex oxides composed of CaO, SiO₂,

Al_2O_3 , and MgO . Figure 1a–c represents the typical inclusions in the initial samples, which exhibited irregular shapes with uneven edges. Figure 1d–f shows the typical inclusions in group R1, which had relatively regular elliptical shapes. Figure 1g–i depicts the typical inclusions in group R2, which exhibited elliptical shapes. Figure 1j–l displays the typical inclusions in group R3, which had regular circular shapes. Figure 1m–o presents the typical inclusions in group R4, which were primarily characterized by irregular circular shapes with uneven edges. Figure 1p–r illustrates the typical inclusions in group R5, which had relatively regular circular shapes with well-defined edges. The surface scan results of the typical inclusions in the H13 steel are shown in Figure 2. It can be seen that the inclusions were mainly composed of Ca, Al, Si, Mg, and O elements, and the elements in the inclusions were uniformly distributed, without delamination.

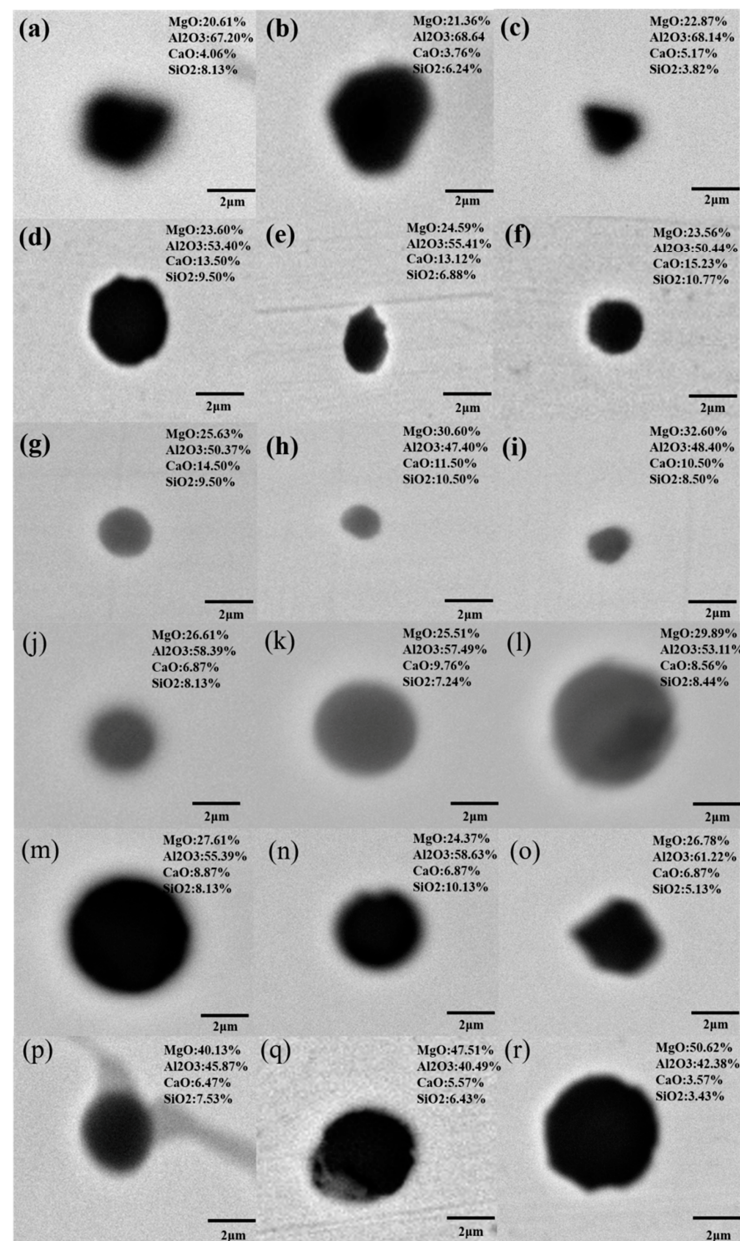


Figure 1. Morphologies and composition distributions of the typical inclusions in the steel samples: (a–c) initial sample; (d–f) R1; (g–i) R2; (j–l) R3; (m–o) R4; and (p–r) R5.

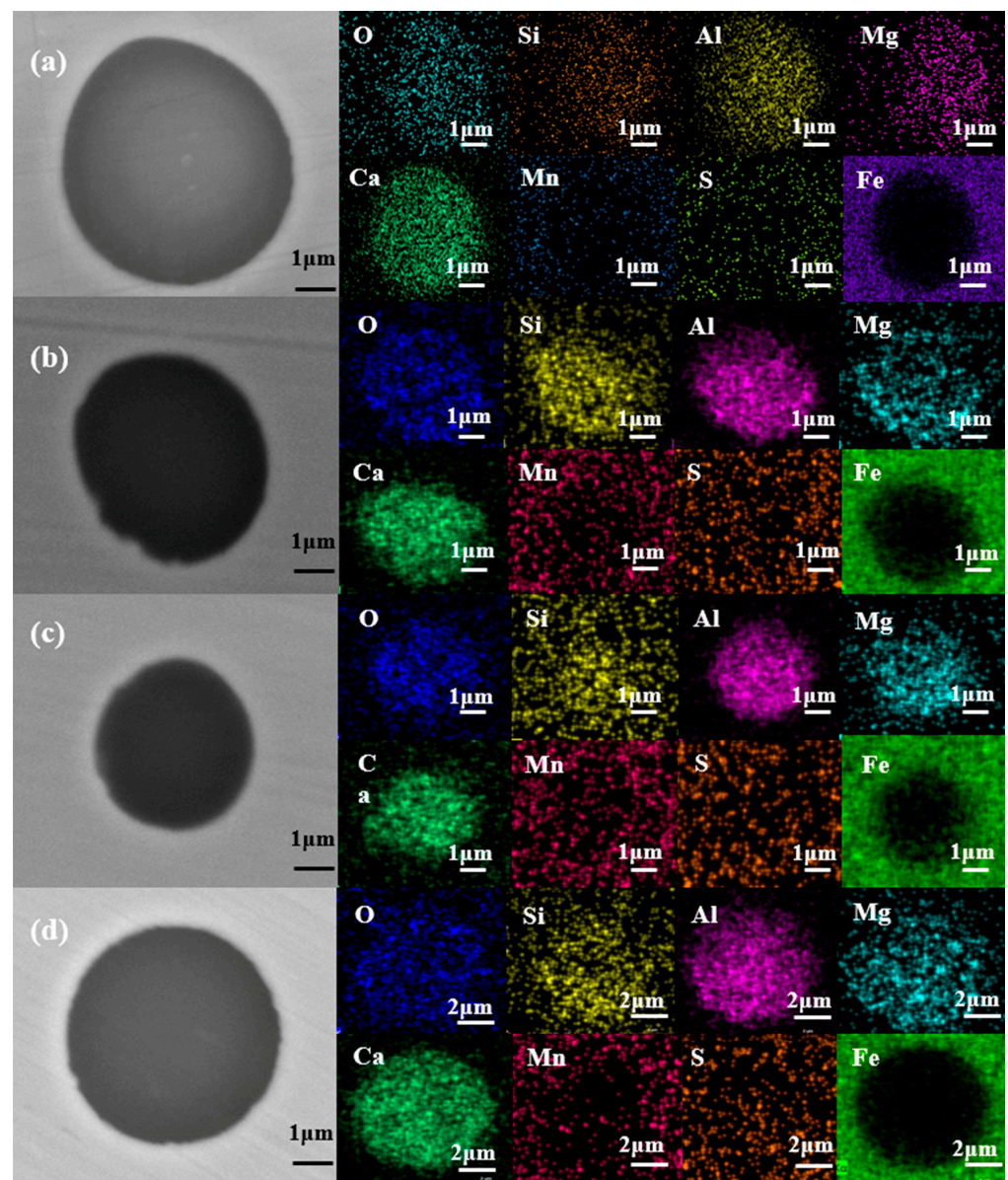


Figure 2. Surface scan of the typical inclusions in the H13 steel. (a) R1, (b) R2, (c) R3, (d) R4.

3.2. Numbers and Sizes of Inclusions

Figure 3 shows the quantitative densities of the inclusions in the steel before and after the reaction of the steel slag. As can be seen from the figure, the number density of the inclusions in the initial steel sample was 40. After reacting with the refining slag, the number densities of the inclusions in the steel samples decreased. With increases in the basicity of the refining slag, the number densities of the inclusions in the steel samples decreased when the C/A was the same, and they were 35, 30, and 25, respectively. When the basicity of the refining slag was the same, the number densities of the inclusions in the steel samples decreased at first and then remained unchanged with the increases in the C/A, which were 32, 30, and 30, respectively. Among these, when the basicity was 6.0 and the C/A was 2.1, the number density of the inclusions in the steel sample was the lowest (i.e., 25).

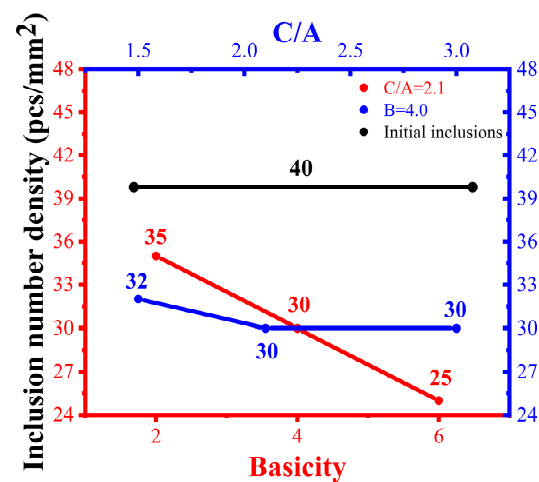


Figure 3. Number densities of the inclusions in the steel samples.

Figure 4 shows the changes in the average sizes of the inclusions in the steel samples before and after the reactions between the H13 steel and the refining slag. It can be seen from the figure that before the reaction between the H13 steel and the refining slag, the average size of inclusions in the initial steel sample was 2.83 μm . After reacting with the refining slag, when the refining slag C/A was the same, the average sizes of inclusions in the steel samples decreased gradually with the increases in the basicity of the refining slag, with values of 2.23 μm , 1.23 μm , and 1.15 μm , respectively. When the basicity of the refining slag was the same, the average sizes of the inclusions in the steel samples decreased at first and then increased with the increases in the refining slag C/A, with values of 1.59 μm , 1.23 μm , and 1.38 μm , respectively. Among these, when the basicity was 6.0 and the C/A was 2.1, the average size of the inclusions in the steel sample was 1.15 μm .

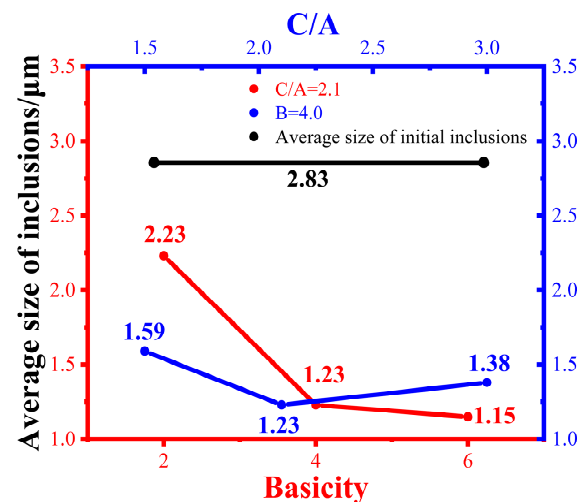


Figure 4. Average sizes of the inclusions in the steel samples.

3.3. Compositions and Plasticities of the Steel Inclusions

By comparing the average content of each component in the inclusions in the steel samples, the relationship between the average content of each component in the inclusions and the basicity and C/A ratio of the refining slag before and after the slag reaction could be explored. Therefore, the variations in the average contents of each component in the inclusions in the steel samples after the slag reactions are plotted in Figure 5. When the refining slag C/A was the same and the basicity was increased, the contents of CaO and Al_2O_3 in the inclusions increased, with the CaO contents increasing from 12% to 15% and the Al_2O_3 contents increasing from 46% to 54%. On the other hand, the contents of

SiO₂ and MgO decreased, with the SiO₂ contents decreasing from 9% to 5% and the MgO contents decreasing from 33% to 26%. When the basicity of the refining slag was the same and the C/A ratios were increased, the contents of CaO, SiO₂, and MgO in the inclusions increased, with the CaO contents increasing from 7% to 13%, the SiO₂ contents increasing from 6% to 8%, and the MgO contents increasing from 30% to 38%. However, the contents of Al₂O₃ decreased from 57% to 42%. The variation trends of the CaO, Al₂O₃, SiO₂, and MgO contents in the inclusions were consistent with the variation trends of the CaO, Al₂O₃, SiO₂, and MgO contents in the refining slag.

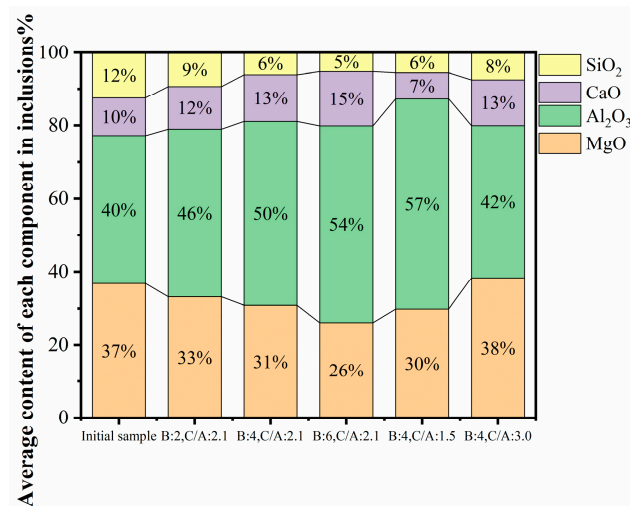


Figure 5. Average contents of each component in the inclusions before and after the steel slag reaction.

The Young's modulus (E) refers to the ratio of stress to strain within the elastic deformation range of a material. When the external stress applied to an inclusion exceeds its elastic limit, plastic deformation occurs. The deformation of an oxide is related to its Young's modulus and hardness value. Therefore, the Young's moduli of non-metallic inclusions can be used to measure their plastic deformation abilities. The larger the Young's modulus of an inclusion, the poorer its plastic deformation ability. The formulas for calculating the Young's modulus E are shown in Equations (1) and (2) [24]:

$$E = 39811V^{-2.9} \text{ and} \quad (1)$$

$$V = M/(\rho n). \quad (2)$$

In Equations (1) and (2), E represents the Young's modulus in GPa, V represents the average atomic volume in $10^{-6} \text{ m}^3/\text{mol}$, M represents the molar mass in kg/mol, ρ represents the density in kg/m^3 , and n represents the number of atoms in the oxide.

In theory, when a slag reaction reaches equilibrium, the composition of an inclusion in the steel is similar to that of the refining slag. Therefore, a Young's modulus map of inclusions could be plotted based on Equations (1) and (2). Figure 6 shows that a higher Al₂O₃ content in an inclusion led to a larger Young's modulus, indicating poorer plastic deformation ability. Thus, it is advisable to minimize the Al₂O₃ contents in slag to enhance the elastic deformation abilities of the inclusions in the steel. From the figure, it can be observed that the Young's moduli of the inclusions in the steel increased with increasing the basicity of the refining slag.

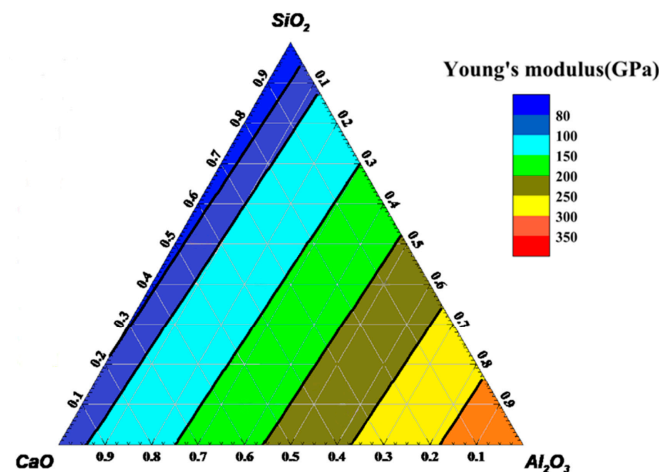


Figure 6. Diagram of the Young's moduli of the inclusions in the CaO-SiO₂-Al₂O₃-6%MgO quaternary slag system.

3.4. Steel-Slag-Inclusion Reaction

The activity lines of the Al₂O₃ in the CaO-SiO₂-Al₂O₃-6%MgO quaternary slag system at 1600 °C were plotted using FactSage 7.2, as shown in Figure 7. It can be seen from the diagram that when the basicity of the refining slag was the same, the activity of the Al₂O₃ in the refining slag decreased with the increases in the refining slag C/A contents. Similarly, when the C/A in the refining slag was the same, the activity of the Al₂O₃ in the refining slag also decreased with the increases in the basicity of the refining slag, but the basicity of the refining slag had relatively little effect on the Al₂O₃ activity in the refining slag. Because Al₂O₃ inclusion has a great influence on the properties of H13 steel, the activity of Al₂O₃ in refining slag can be reduced by increasing the C/A of the refining slag, and the content of Al in the molten steel can be reduced and, thus, the content of Al₂O₃ in the inclusion can be reduced and the properties of H13 steel can be improved. Therefore, the proportion of Al₂O₃ in refining slag should not be too high.

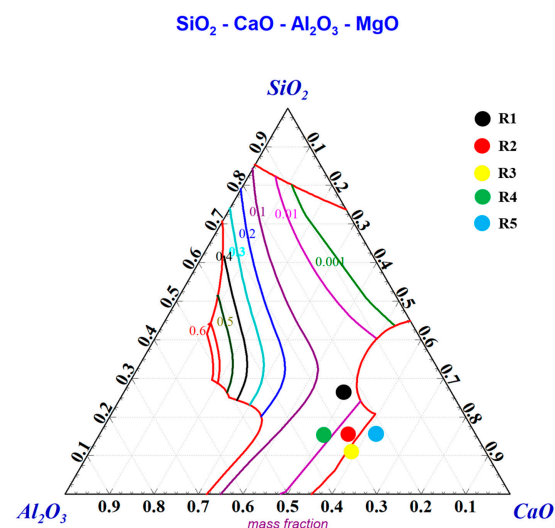


Figure 7. Al₂O₃ isoactivity lines of the CaO-SiO₂-Al₂O₃-6% MgO slag system.

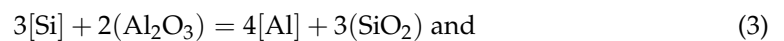
Equilibrium experiments on steel-slag reactions were conducted using the designed five sets of refining slag systems, and the Al contents in the steel were measured using an ICP-OES instrument. It can be seen from the Table 3 that the initial Al content in the steel sample was 40 ppm. The contents of Al in the steel samples increased after the reaction between the H13 steel and the refining slag. When the basicity of the refining slag was the same, the contents of Al in the steel samples decreased with the increases in the refining

slag C/A, with values of 197 ppm, 116 ppm, and 92 ppm, respectively. When the refining slag C/A was the same, the content of Al in the steel samples increased with the basicity of the refining slag, with values of 104 ppm, 116 ppm, and 136 ppm, respectively.

Table 3. Al contents in the molten steel samples for the equilibrium of steel slag reactions (ppm).

Experiment Number	R1	R2	R3	R4	R5
Al content	104	116	136	197	92

By investigating the variations in the Al_2O_3 contents in the five sets of refining slag samples and the Al contents in the steel melt samples, the relationship between the Al contents in the steel melt and the Al_2O_3 contents in the refining slag was plotted. As shown in Figure 8, the Al contents in the steel melt increased with increasing the Al_2O_3 contents in the slag and vice versa. Among these, the highest Al_2O_3 content was found in R4, reaching 29.6% and corresponding to the highest Al content of 197 ppm. The increase in the Al content in the steel melt could be explained by Equations (3) and (4), where the Si in the steel melt reduced the Al_2O_3 in the slag to Al. With a sufficient amount of Si in the steel melt, the Al content in the steel melt increased with the increasing Al_2O_3 contents in the slag. In the experiment where we pre-melted the slag with an Al_2O_3 crucible, the content of Al_2O_3 in the slag increased because the Al_2O_3 crucible was eroded by the slag, thus increasing the content of Al_2O_3 in the slag. However, this paper does not further explore the principle of erosion.



$$\Delta G = -641620.73 + 95T. \quad (4)$$

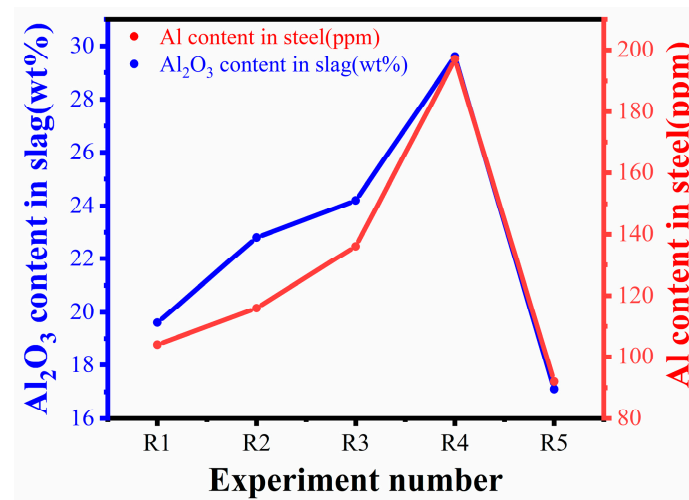


Figure 8. Relationship between the Al_2O_3 content in refining slag and the Al content in molten steel.

Figure 9 shows the relationship between the Al content in the steel melt and the inclusion mass calculated using FactSage 7.2. It can be observed that with the increases in the Al content in the steel melt, the masses of the inclusions in the steel melt gradually decreased. The experimental measurements of the inclusion densities and sizes also decreased with increasing the basicity and C/A ratio. In other words, as the Al contents in the steel melt increased, the masses of the inclusions decreased, which was consistent with the calculated results.

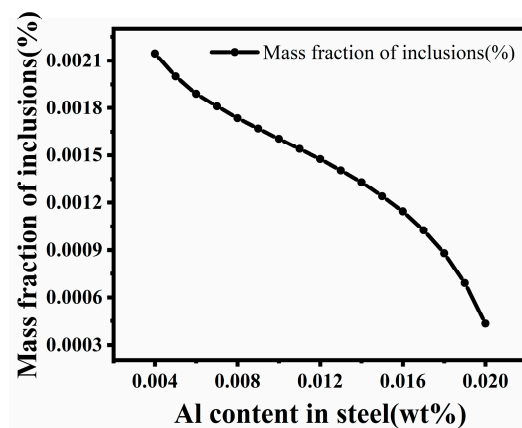


Figure 9. Relationship between Al content and inclusion quality in molten steel.

Figure 10 presents the relationship between the Al content in the steel melt and the inclusion composition calculated using FactSage 7.2. It can be observed that with the increases in the Al contents in the steel melt, the compositions of the inclusions in the steel melt also changed. The Al_2O_3 contents in the inclusions increased from 39% to 62% with increasing Al contents while the SiO_2 contents decreased from 20% to 11%. The CaO contents initially increased from 12% to 17% and then decreased to 11% with the increasing Al contents. The MgO contents initially decreased from 26% to 18% and then increased to 20% with the increasing Al contents. Combined with the experimental measurements of inclusion compositions, the calculated results showed the same trends as the experimental results.

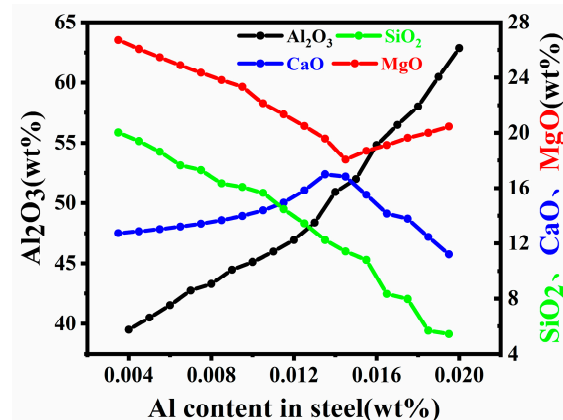


Figure 10. Effect of Al content in molten steel on inclusion composition.

4. Conclusions

In this study, a high basicity (2.0~6.0) and high $\text{CaO}/\text{Al}_2\text{O}_3$ ratio (1.5~3.0) fluorine-free $\text{CaO}-\text{Al}_2\text{O}_3-\text{SiO}_2-\text{MgO}$ quaternary refining slag was used. By conducting high-temperature steel-slag experiments combined with the thermodynamic software FactSage and analyzing the experimental results and calculations, the influence of this slag system on the morphologies, compositions, and quantities of the inclusions in the steel was investigated. The below conclusions were drawn.

With the increase in slag basicity from 2.0 to 6.0, the shapes of the inclusions changed from elliptical to regular and circular. When the $\text{CaO}/\text{Al}_2\text{O}_3$ ratio in the slag system was 1.5, the inclusions had irregular and circular morphologies which became regular when the $\text{CaO}/\text{Al}_2\text{O}_3$ ratio increased to 3.

- (1) As the slag basicity and the $\text{CaO}/\text{Al}_2\text{O}_3$ ratio increased, the densities of the inclusions decreased, and the sizes of the inclusions in the steel decreased with increasing the

slag basicity. When the slag basicity was constant, the sizes of the inclusions decreased with increasing the CaO/Al₂O₃ ratio, and then they increased. Overall, the best control effect on the inclusion density and size was achieved when the slag basicity was 6 and the CaO/Al₂O₃ ratio was 2.1. The inclusion density was 25 per mm², and the size could reach 1.15 μm.

- (2) By comparing the average contents of each component in the inclusions in the steel samples, it was found that the variations in the CaO, Al₂O₃, SiO₂, and MgO contents in the inclusions were consistent with the variations in the CaO, Al₂O₃, SiO₂, and MgO contents in the refining slag. The Al₂O₃ contents in the slag increased with increasing the slag basicity, and they decreased with increasing the CaO/Al₂O₃ ratio. According to the calculated results, reducing the Al₂O₃ contents in the slag and inclusions was beneficial for reducing the moduli of elasticity of the inclusions and improving their abilities for elastic deformation. With the increases in slag basicity, the moduli of elasticity of the inclusions showed an increasing trend.
- (3) In combining the experimental results and calculation analysis, it was found that with the increases in the CaO/Al₂O₃ ratios in the slag system, the Al contents in the steel melt decreased, and the masses of the inclusions decreased. The Al contents in the steel melt also affected the compositions of the inclusions. With the increases in the Al contents in the steel melt, the Al₂O₃ contents in the inclusions increased from 39% to 62% while the SiO₂ contents decreased from 20% to 11%. The CaO contents initially increased from 12% to 17% with increasing the Al contents, and then they decreased to 11%. The MgO contents initially decreased from 26% to 18% and then increased to 20% with increasing the Al contents.

Author Contributions: T.L., Z.Q. and L.W. Conceptualization, methodology, T.L.; software, Z.Q.; writing—original draft preparation, L.W.; Funding Acquisition, Resource, Supervision, T.L., Z.Q. and L.W.; writing—review and editing. All authors have read and agreed to the published version of the manuscript.

Funding: This research received no external funding.

Data Availability Statement: Data available on request due to restrictions eg privacy or ethical. The data presented in this study are available on request from the corresponding author. The data are not publicly available due to privacy.

Acknowledgments: This research was supported by the National Natural Science Foundation of China (Grant Nos. 52064011 and 52274331), Guizhou Provincial Basic Research Program (Natural Science) (Nos. ZK [2021]258, ZK [2022] Zhongdian 023 and ZK [2023] Zhongdian 020), Guizhou Provincial Program on Commercialization of Scientific and Technological Achievements (No [2022]089).

Conflicts of Interest: The authors declare no conflict of interest.

References

1. Wegener, T.; Krochmal, M.; Möller, T.R.; Le, M.T.; Czap, A.; Marianek, F.; Fakesch, H.; Niendorf, T. On the low-cycle fatigue behavior of a novel high strength mold steel. *Int. J. Fatigue* **2023**, *175*, 107754. [[CrossRef](#)]
2. Zhou, Y.; Chen, L.; Jiang, W.; Cui, S.; Cui, X. Investigation on elevated-temperature wear performance and wear failure mechanism of a tungsten-system hot-working die steel. *Surf. Topogr. Metrol. Prop.* **2022**, *10*, 035007.
3. Li, X.; Jiang, Z.; Geng, X.; Chen, M.; Peng, L. Evolution mechanism of inclusions in H13 steel with rare earth magnesium alloy addition. *ISIJ Int.* **2019**, *59*, 1552–1561. [[CrossRef](#)]
4. Jiang, Q.C.; Sui, H.L.; Guan, Q.F. Thermal fatigue behavior of new type high-Cr cast hot work die steel. *ISIJ Int.* **2004**, *44*, 1103–1107. [[CrossRef](#)]
5. Fuchs, D.; Tobie, T.; Stahl, K. Challenges in determination of microscopic degree of cleanliness in ultra-clean gear steels. *J. Iron Steel Res. Int.* **2022**, *29*, 1583–1600. [[CrossRef](#)]
6. Sahai, Y. Tundish technology for casting clean steel: A review. *Metall. Mater. Trans. B* **2016**, *47*, 2095–2106.
7. Wang, Z.; Guan, Y.H.; Luo, H.W. Progress on statistical models of evaluating inclusions in clean steels. *J. Iron Steel Res. Int.* **2022**, *29*, 1153–1163.
8. Tridello, A.; Paolino, D.S.; Chiandussi, G.; Rossetto, M. VHCF strength decrement in large H13 steel specimens subjected to ESR process. *Procedia Struct. Integr.* **2016**, *2*, 1117–1124.

9. Liu, X.; Yang, J.; Zhang, F.; Fu, X.; Li, H.; Yang, C. Experimental and DFT study on cerium inclusions in clean steels. *J. Rare Earths* **2021**, *39*, 477–486.
10. Mapelli, C. Control and engineering of non-metallic inclusions belonging to x₂o(2)center dot ycao center dot zal(2)o(3) system in ca-treated al-killed and al-si-killed steel. *Steel Res. Int.* **2006**, *77*, 462–471.
11. Krajnc, L.; Burja, J.; Medved, J.; Kim, T.S.; Park, J.H. Formation behaviour of spinel-cas multiphase inclusions in ca-treated resulphurised steel during the ladle furnace process. *Mater. Tehnol.* **2020**, *54*, 559–565. [[CrossRef](#)]
12. Xiao, G.H.; Dong, H.; Wang, M.Q.; Hui, W.J. Hot deformability of oxide-sulfide duplex inclusions in calcium-treated gear steels. *Beijing Keji Daxue Xuebao/J. Univ. Sci. Technol. Beijing* **2010**, *32*, 735–738.
13. Gollapalli, V.; Rao, M.B.V.; Karamched, P.S.; Borra, C.R.; Roy, G.G.; Srirangam, P. Modification of oxide inclusions in calcium-treated al-killed high sulphur steels. *Ironmak. Steelmak.* **2018**, *46*, 663–670. [[CrossRef](#)]
14. Li, Y.; Yang, H.; Jiang, Z.H.; Li, H.B.; Sun, M.; Ma, S. Change of Spinel in High Ca Treatment at 38CrMoAl Steel. *ISIJ Int.* **2022**, *62*, 2276–2285. [[CrossRef](#)]
15. Wang, Y.; Sun, X.; Zhang, L.; Ren, Y. Effect of calcium treatment on inclusions in Si-Mn-killed 304 stainless steels. *J. Mater. Res. Technol.* **2020**, *9*, 11351–11360. [[CrossRef](#)]
16. Sun, H.; Yang, J. Evolution behaviour and modification mechanism of inclusions in NM500 wear-resistant steel with calcium treatment. *Ironmak. Steelmak.* **2022**, *49*, 795–812. [[CrossRef](#)]
17. Wang, W.; Zhang, L.; Luo, Y.; Ren, Y.; Sun, X. Transformation of inclusions in Al-killed steels with different calcium contents during the heat treatment. *Ironmak. Steelmak.* **2022**, *49*, 472–483. [[CrossRef](#)]
18. Bielefeldt, W.V.; Vilela, A.C.F. Computational thermodynamic study of inclusions formation in the continuous casting of SAE 8620 steel. *Steel Res. Int.* **2010**, *81*, 1064–1069. [[CrossRef](#)]
19. Guo, J.; Cheng, S.S.; Cheng, Z.J. Characteristics of Deoxidation and Desulfurization during LF Refining Al-killed Steel by Highly Basic and Low Oxidizing Slag. *J. Iron Steel Res. Int.* **2014**, *21*, 166–173. [[CrossRef](#)]
20. Liu, J.; Li, B.; Jia, Y.; Chen, J.; Feng, J.; Ren, B.; Gong, D. Slag resistance mechanism of CaO 6Al₂O₃ refractory and its effect on inclusions of aluminum deoxidized steel. *Int. J. Appl. Ceram. Technol.* **2022**, *19*, 3323–3333. [[CrossRef](#)]
21. Wang, Y.; Yang, S.; Li, J.; Wang, F.; Gu, Y. Cyclic use of ladle furnace refining slag for desulfurization. *J. Sustain. Metall.* **2017**, *3*, 274–279. [[CrossRef](#)]
22. Zhang, H.; Liu, C.; Lin, Q.; Wang, B.; Liu, X.; Fang, Q. Formation of plastic inclusions in U71Mnk high-speed heavy-rail steel refined by Cao-Si₂-Al₂O₃-MgO slag. *Metall. Mater. Trans. B* **2019**, *50*, 459–470. [[CrossRef](#)]
23. Wu, Z.; Li, J.; Shi, C.; Du, G. Effect of MgO content in slag system on inclusions in magnesium aluminum iron alloy deoxygenated H13 steel. *Mech. Eng. Mater.* **2015**, *39*, 5–10.
24. Zhang, R.; Zhang, Z. Research and Application of Desulfurization in LF Refining Furnace at Taigang Steelmaking Plant. In Proceedings of the 2009 Shandong Metallurgical Society Steelmaking Academic Exchange Conference, Shandong, China, 1 September 2009; pp. 112–114.
25. Li, Y.; Liu, M.; Liu, X. Production Process Practice of H13 Mold Steel Ingots. In Proceedings of the 2009 Shandong Metallurgical Society Steelmaking Academic Exchange Conference, Shandong, China, 1 September 2009; pp. 28–30.
26. Huang, T.; Bi, S.; Zhang, W. LF+VD Outside Furnace Refining Technology for Clean Steel Production. In Proceedings of the 2012 Steelmaking Continuous Casting High Quality Clean Steel Production Technology Exchange Conference, Liaoning, China, 1 September 2012; pp. 66–70.
27. Yang, W.; Wang, S.; Yun, X. Analysis and Research on the Resource Utilization of LF Furnace Refining Slag. In Proceedings of the 2021 Science and Technology Annual Meeting of the Chinese Society for Environmental Sciences (II), Tianjin, China, 19 October 2021; pp. 711–718.
28. Yang, H.; Su, L.; Li, G.; Chen, Z.; Pi, C.; Zhou, Y. The effect of refining slag on inclusions in SUS444 ferritic stainless steel. *Steelmaking* **2014**, *30*, 42–4651.
29. Ruan, X.; Jiang, Z.; Gong, W.; Li, Y.; Li, J. The effect of refining slag on oxygen content and inclusions in bearing steel. *Spec. Steel* **2008**, *29*, 1–3.
30. Wang, Y.; Fu, G.; Li, Z. Research on the effect of high basicity refining slag on the inclusion characteristics of GCr15 bearing steel. *Hebei Metall.* **2018**, *12*, 13–16.
31. Yu, H.; Qiu, G.; Hao, L.; Zhao, Y.; Wang, X. Refining slag Al₂O₃ Effect of Content on Inclusions in Aluminum Deoxidized Steel. *Steelmaking* **2023**, *39*, 18–23.
32. Ji, Y.; Liu, C.; Lu, Y.; Yu, H.; Huang, F.; Wang, X. Effects of FeO and CaO/Al₂O₃ ratio in slag on the cleanliness of Al-killed steel. *Metall. Mater. Trans. B* **2018**, *49*, 3127–3136. [[CrossRef](#)]
33. Ma, W.J.; Bao, Y.P.; Wang, M.; Zhao, D.W. Influence of slag composition on bearing steel cleanness. *Ironmak. Steelmak.* **2014**, *41*, 26–30. [[CrossRef](#)]

Disclaimer/Publisher's Note: The statements, opinions and data contained in all publications are solely those of the individual author(s) and contributor(s) and not of MDPI and/or the editor(s). MDPI and/or the editor(s) disclaim responsibility for any injury to people or property resulting from any ideas, methods, instructions or products referred to in the content.